Regular Article

blood

THROMBOSIS AND HEMOSTASIS

A mechanistic investigation of thrombotic microangiopathy associated with IV abuse of Opana ER

Ryan Hunt,[1,*] Ayla Yalamanoglu,[2,*] James Tumlin,[3] Tal Schiller,[1] Jin Hyen Baek,[2] Andrew Wu,[1] Agnes B. Fogo,[4] Haichun Yang,[4] Edward Wong,[5-7] Peter Miller,[8-10] Paul W. Buehler,[2] and Chava Kimchi-Sarfaty[1]

[1]Division of Plasma Protein Therapeutics, Office of Tissues and Advanced Therapies and [2]Division of Blood Components and Devices, Office of Blood Research and Review, Center for Biologics Evaluation and Research, US Food and Drug Administration, Silver Spring, MD; [3]Department of Internal Medicine, University of Tennessee College of Medicine at Chattanooga, Chattanooga, TN; [4]Department of Pathology, Microbiology, and Immunology, Vanderbilt University Medical Center, Nashville, TN; [5]Department of Pediatrics and [6]Department of Pathology, George Washington School of Medicine and Health Sciences, Washington, DC; [7]Department of Coagulation, Quest Diagnostics/Nichols Institute, Chantilly, VA; and [8]Section on Hematology and Oncology, Department of Internal Medicine, [9]Section on Pulmonary, Critical Care, Allergy and Immunology, and [10]Section on Critical Care Medicine, Department of Anesthesiology, Wake Forest School of Medicine, Winston-Salem, NC

Key Points

- The inert ingredients in Opana ER tablets can elicit TMA in the setting of IV abuse and stems from the impact of HMW PEO.

Since 2012, a number of case reports have described the occurrence of thrombotic microangiopathy (TMA) following IV abuse of extended-release oxymorphone hydrochloride (Opana ER), an oral opioid for long-term treatment of chronic pain. Here, we present unique clinical features of 3 patients and investigate IV exposure to the tablet's inert ingredients as a possible causal mechanism. Guinea pigs were used as an animal model to understand the hematopathologic and nephrotoxic potential of the inert ingredient mixture (termed here as PEO+) which primarily contains high-molecular-weight polyethylene oxide (HMW PEO). Microangiopathic hemolytic anemia, thrombocytopenia, and acute kidney injury were found in a group of 3 patients following recent injection of adulterated extended-release oxymorphone tablets. Varying degrees of cardiac involvement and retinal ischemia occurred, with TMA evident on kidney biopsy. A TMA-like state also developed in guinea pigs IV administered PEO+. Acute tubular and glomerular renal injury was accompanied by nonheme iron deposition and hypoxia-inducible factor-1α upregulation in the renal cortex. Similar outcomes were observed following dosing with HMW PEO alone. IV exposure to the inert ingredients in reformulated extended-release oxymorphone can elicit TMA. Although prescription opioid abuse shows geographic variation, all physicians should be highly inquisitive of IV drug abuse when presented with cases of TMA. (*Blood.* 2017;129(7):896-905)

Introduction

Prescription opioids are effective analgesics in the setting of severe and chronic pain but carry a high potential for dependency and abuse. In geographically defined areas of the United States, the prevalence of abuse has reached epidemic proportions and represents a serious public health concern.[1] The adulteration of prescription opioids commonly involves crushing, heating, and liquid extraction of tablets followed by nasal inhalation or injection. A 2013 Centers for Disease Control and Prevention (CDC) Morbidity and Mortality Weekly Report first described the occurrence of a "thrombotic thrombocytopenic purpura (TTP)–like illness" of unclear etiology in patients who had recently injected adulterated tablets of extended-release oxymorphone hydrochloride.[2] A number of case reports have subsequently emerged describing patients with microangiopathic hemolytic anemia, thrombocytopenia, and renal failure,[3-8] with thrombotic microangiopathy (TMA) observed in kidney biopsies. These individuals commonly present with sequelae related to injection drug abuse. Soft tissue, musculoskeletal, and blood-borne infection have been diagnosed even in the absence of overt TMA. A 2015 outbreak of HIV in rural Indiana, where a majority of infected persons reported injecting "melted" tablets of extended-release oxymorphone, speaks to this trend.[9]

Syndromes of TMA include a variety of pathogenic mechanisms with unique approaches to care.[10] TTP arises through a severe deficiency of ADAMTS13, the von Willebrand Factor (VWF)-cleaving protease.[11-13] The accumulation of ultra-large VWF multimers promotes the deposition of platelet-rich thrombi within the microcirculation.[14] Other TMA syndromes arise independent of changes to ADAMTS13 and encompass complement-, toxin- and drug-mediated syndromes. Significant deficiencies of ADAMTS13 have not been found in patients with TMA associated with IV abuse of extended-release oxymorphone, although not all individuals were tested. Approaches to treatment have ranged from early plasma exchange therapy to aggressive supportive care alone,[4] but the mechanistic basis for these cases of TMA remains unclear.

In early 2012, Endo Pharmaceuticals reformulated tablets of extended-release oxymorphone to contain a crush-resistant ingredient mixture. The formulation is chiefly composed of high-molecular-weight

Submitted 31 August 2016; accepted 7 November 2016. Prepublished online as *Blood* First Edition paper, 18 November 2016; DOI 10.1182/blood-2016-08-736579.

*R.H. and A.Y. contributed equally to this study.

The online version of this article contains a data supplement.

There is an Inside *Blood* Commentary on this article in this issue.

The publication costs of this article were defrayed in part by page charge payment. Therefore, and solely to indicate this fact, this article is hereby marked "advertisement" in accordance with 18 USC section 1734.

polyethylene oxide (HMW PEO; ~7 000 000 Da) in addition to smaller amounts of hypromellose, macrogol, α-tocopherol, and citric acid: herein collectively referred to as PEO+. The US Food and Drug Administration (FDA) determined that the reformulated tablet may indeed "resist crushing relative to the original formulation" but can be "readily prepared for injection."[15] The true epidemiologic impact of the reformulation remains uncertain, and the tablet currently does not have abuse-deterrent labeling. The hematotoxic potential of IV HMW PEO has received limited attention. An abrupt lethal effect of IV HMW PEO was described in animals shortly after the first synthesis of the polymer[16] and rats administered IV or intraperitoneal HMW PEO have been reported to develop hemolytic anemia.[17]

Here, we describe illustrative cases of TMA in patients exposed to PEO+ during IV abuse of extended-release oxymorphone tablets. We next evaluate the dose-dependent effects of IV PEO+ administration in guinea pigs. We show that the inert ingredients generate acute hematotoxicity and kidney injury, consistent with a mechanistic link between the tablet's constituents and cases of TMA following its IV abuse in humans.

Methods

In vivo administration of IV PEO+

Male Hartley guinea pigs (Charles River Laboratories) were maintained in the animal facility of the FDA Center for Biologics Evaluation and Research (CBER) Animal Care Facility. Animals were 8 to 10 weeks old and weighed 650 to 850 g before surgery. Animal protocols were approved by the FDA CBER Institutional Animal Care and Use Committee, and all experimental procedures were performed in compliance with the National Institutes of Health guidelines on the use of experimental animals. The inert ingredient mixture was provided by Endo Pharmaceuticals under a research collaborative agreement. The bulk PEO+ powder was dissolved in 1× phosphate-buffered saline by heating to 45°C with gentle agitation to achieve a 1 mg/mL stock solution. To achieve solution consistency, the solubilized material was centrifuged at 10 000*g* for 20 minutes to remove large undissolved aggregates. Bolus injections were administered via an indwelling jugular catheter. Blood samples were obtained at baseline, 4, 8, 24, and 48 hours and animals were euthanized at 24 or 48 hours after initial injection for tissue collection and histopathologic examination.

Hematological analysis

Blood samples were collected into heparin-containing tubes at indicated time points via an indwelling jugular catheter. Peripheral blood smears were prepared and red blood cell (RBC) count, hematocrit, and platelet count were determined using a Cell-Dyn 3700 hematology analyzer (Abbott Diagnostics) in veterinary mode; a manual white blood cell (WBC) count and differential were performed. Plasma was prepared by centrifugation of whole blood at 1500*g* for 10 minutes and stored at −80°C.

Analysis of acute kidney injury

NGAL quantitative RT-PCR. Total RNA was isolated from guinea pig kidney cortical tissue using a TRIzol isolation protocol followed by complementary DNA synthesis (Applied Biosystems). Quantitative real-time polymerase chain reaction (RT-PCR) was performed on a LightCycler 480 (Roche) using TaqMan Universal PCR Master Mix and the following TaqMan primer/probes for guinea pig Lcn2 (neutrophil gelatinase-associated lipocalin [NGAL]) (forward, 5′-GTCCCACCACTGAGCAAGAT-3′; reverse, 5′-GTCATCTTTCAGCCCGTAGG-3′; TaqMan probe, 5′-CAAGACAAGT TCCAGGGGAA-3′) and 18S ribosomal RNA (Mm03928990_g1). Samples were assayed in triplicate. Crossing point (Cp) values were obtained and ΔΔCp values were calculated using 18S as the reference gene. Statistical analysis was performed on raw ΔCp data.

Urinary albumin determination. Albumin content in urine was measured using a commercially available guinea pig albumin enzyme-linked immunosorbent assay (ELISA) kit (MyBioSource).

Plasma creatinine measurement. Plasma creatinine levels were determined by a colorimetric assay kit (Abcam).

Sodium dodecyl sulfate–polyacrylamide gel electrophoresis/ Western blot

Tissue lysates were resolved on NuPAGE Novex 4% to 12% Bis-Tris gels (Thermo Fisher), transferred to nitrocellulose membranes, and blocked for 1 hour with 5% nonfat dry milk solution. Membranes were incubated overnight at 4°C in primary antibody solution. Primary antibodies used were mouse anti-hemeoxygenase-1 (Enzo Lifescience), mouse anti-β-actin (Abcam), goat anti–hypoxia-inducible factor 1α (HIF-1α; R&D Systems). Membranes were incubated with horseradish peroxidase (HRP)-conjugated goat anti-mouse (Thermo Fisher) or bovine anti-goat (Santa Cruz Biotechnology) antibodies for 1 hour at room temperature. A chemiluminescent signal was developed using SuperSignal West Pico chemiluminescent substrate (Pierce) and visualized using an Image Station 4000MM Pro (Carestream). Densitometry analysis was performed using Kodak molecular imaging software (Carestream).

Spectrophotometric determination of plasma hemoglobin

Hemoglobin in plasma was measured in semimicro cuvettes using a Cary 60 UV-Vis spectrophotometer (Agilent Technologies). Absorbance was measured between 350 and 650 nm. Spectra were deconvoluted against standard extinction curves of pure substances using a nonnegative least square algorithm.

Measurement of HMW PEO in plasma

The concentration of PEO within plasma of guinea pigs was determined using a Life Diagnostics ELISA kit that recognizes the PEO backbone.

RBC ektacytometry

RBC deformability was measured using ektacytometry (RheoScan-AnD 300; Rheomeditech). The elongation index was evaluated from 0 to 20 Pa and compared at 3 to 9 Pa, which is relevant to shear stress experienced by circulating RBCs.

Tissue iron measurements

Iron content within renal cortex tissue was determined by a ferrozine-based assay as previously described.[18]

Histopathology

Kidney and spleen were fixed in 10% formalin for 24 hours and stored in 100% isopropanol. Tissue was embedded in paraffin, and 2- to 5-μm sections were prepared. Hematoxylin-and-eosin (H&E) and Perls diaminobenzidine (DAB) staining were performed as previously described.[19] Patient kidney biopsy sections were routinely processed for light microscopy with H&E, periodic acid Schiff, and Jones silver staining, immunofluorescence for immunoglobulins IgG, IgA, IgM, κ, λ, and complements C3 and C1q, and for electron microscopy, with scout sections viewed and glomeruli selected for thin sectioning and viewed in a Philipps Morgagni electron microscope.

Immunohistochemistry

Sections were dewaxed and rehydrated. Citrate buffer antigen retrieval was performed by microwave heat treatment of 15 minutes and cooling for 30 minutes at room temperature. Slides were incubated with 3% H_2O_2 for 20 minutes to quench endogenous peroxidase activity. Sections were blocked with 2.5% normal horse serum (Vector Laboratories) for 1 hour at room temperature before overnight incubation at 4°C in primary antibody (mouse anti-polyethylene glycol [clone 3F12-1; Life Diagnostics]) or rabbit anti-fibrinogen (Abcam). After washing, a peroxidase-conjugated anti-mouse IgG reagent or alkaline phosphatase–conjugated anti-rabbit IgG reagent (Vector Laboratories) was added to each slide for 30 minutes at room temperature.

Table 1. Clinical characteristics in 3 patients treated for TMA following IV abuse of extended-release oxymorphone

	Patient 1	Patient 2	Patient 3
Age, y	24	28	48
Sex	Female	Male	Female
Presenting symptoms	Numbness of extremities, vision loss	Angina, dyspnea, abdominal pain, vision loss	Angina, dyspnea, abdominal pain, diarrhea, numbness of extremities, vision loss
Treatment	5 times plasma exchange	9 times plasma exchange	5 times plasma exchange

The peroxidase signal was developed using 3, 3′-DAB or red alkaline phosphatase substrate (Vector Laboratories) and counterstained with Gill II hematoxylin.

VWF multimer analysis

Guinea pig plasma samples or control guinea pig platelet lysate were electrophoresed on a 0.6% agarose–sodium dodecyl sulfate (SDS) gel in a horizontal gel apparatus at 4°C. Electrophoresis was performed until the dye front migrated ~9 cm. Protein was transferred overnight onto an Immobilon-P polyvinylidene difluoride membrane (Millipore) at 100 mA in a *trans*-blot cell tank (Bio-Rad) at 4°C. After blocking in 5% nonfat milk for 1 hour, the membrane was incubated at room temperature for 2 hours with a rabbit anti-VWF polyclonal antibody (Abcam) followed by a HRP-conjugated goat anti-rabbit secondary antibody (Lifespan Bio) for 1 hour. The chemiluminescent signal was developed using SuperSignal West Pico chemiluminescent substrate (Pierce) and visualized using an Image Station 4000MM Pro (Carestream).

VWF antigen and collagen-binding activity

VWF antigen (Abcam) and collagen-binding activity (Technoclone) were determined using commercially available ELISA kits.

Endothelial cell culture

Primary human umbilical vein endothelial cells (HUVECs; Thermo Fisher) were cultured in media supplemented with various amounts of PEO+ or 1 μg/mL lipopolysaccharide (Sigma-Aldrich) for 24 hours. The amount of soluble VCAM (sVCAM) was quantified by ELISA (R&D Systems).

Statistical analysis

Data are presented as mean ± standard error of the mean (SEM) unless otherwise noted. A 1-way analysis of variance (ANOVA) was used to compare means among groups with a Tukey corrected posttest for between group comparisons. $P < .05$ was considered statistically significant. All statistical analyses were performed using GraphPad Prism (version 6.02).

Results

TMA following IV abuse of extended-release oxymorphone in humans

Two female and 1 male patient presented to the emergency department of Erlanger Medical Center in Chattanooga, TN with complaints of chest pain, dyspnea, and varying degrees of visual impairment. Two patients were found to be in acute renal failure and all 3 had anemia and thrombocytopenia. Laboratory data also revealed elevated lactate dehydrogenase (LDH) and undetectable serum haptoglobin levels (Tables 1 and 2). Examination of peripheral blood smears showed microspherocytosis, schistocytosis (>10%), and markedly reduced platelets: features consistent with microangiopathic hemolytic anemia. At presentation, 2 of 3 patients had reductions in C3 and C4 serum complements. Troponin levels were elevated in all 3 patients and an electrocardiogram in the male patient revealed diffuse ST segment elevation and PR segment depression, consistent with acute pericarditis. An echocardiogram in this patient showed reduced left ventricular and right ventricular function (ejection fraction of 30%) but no overt pericardial effusion. Percutaneous coronary intervention was not performed due to the likelihood of a microvascular disease process. Dyspnea was associated with diffuse alveolar infiltrates on chest radiograph.

Based upon these findings, the patients were initiated on plasma exchange therapy until ADAMTS13 levels could be determined. The male patient also required acute hemodialysis throughout his hospitalization. Gelatinous material within patient plasma was found to occlude the dialysis catheter, pheresis tubing, and bedside drain. Upon further questioning, all 3 patients reported recent IV abuse of extended-release oxymorphone tablets. According to the account of the male patient, as many as 10 extractions had been performed on a single tablet with the last injection occurring ~6 hours prior to presentation. Kidney biopsies were performed in 2 patients and showed TMA, dominantly affecting arterioles and interlobular arteries with focal endothelial swelling involving larger arteries, accompanied by extensive acute tubular injury (Figure 1A-B). There were no immune complexes seen by immunofluorescence. Transmission electron microscopy showed increased lamina rara interna, podocyte foot process effacement, and cellular vacuolization with no deposits (Figure 1C-D). The clearance of gelatinous material continued through the first 3 plasma exchange sessions and then began to diminish. Plasma exchange was continued through at least 5 cycles, and all patients demonstrated complete or partial recovery of renal function prior to discharge. Over the first 3 days, the loss of vision worsened in all 3 patients with the male patient developing near total blindness in the left eye and marked reduction of visual acuity in the right. An ophthalmologic examination and fluorescence angiography revealed diffuse occlusive disease of retinal arterioles (Figure 1E). The male patient was discharged with chronic renal disease (serum creatinine, 2.3 mg/dL) and unfortunately continued to IV abuse Opana ER tablets. He was admitted a second time with TMA and became hemodialysis-dependent. With continued abuse, he eventually died ~18 months after his initial presentation. The other 2 patients were not readmitted and lost to follow-up.

The potential for excipients in extended-release oxymorphone to cause TMA when IV administered to guinea pigs

To guide our investigation, we first determined the amount of inert ingredients (termed here PEO+) that would be extracted and delivered through a typical adulteration process. Tablets (40 mg) were cut into 4 to 5 pieces and heated together on a spoon in 2 mL of water to the point of boiling with a propane torch. When the volume was reduced by ~50%, the remaining liquid was collected. Through 5 extractions of a single 40-mg tablet, the total mass of the dried excipients was ~14 mg. Assuming complete distribution within the plasma volume of a 70-kg adult, the resulting plasma concentration of PEO+ would be ~5 μg/mL.

To account for variation in injection frequency and adulteration method, we sought to achieve a range of PEO+ levels within blood by establishing 4 IV dosing schemes: 0.1 mg/kg or 0.3 mg/kg bolus

Table 2. Laboratory abnormalities in 3 patients treated for TMA following IV abuse of extended-release oxymorphone

	Patient 1		Patient 2		Patient 3	
Test result	**Presentation**	**Peak or nadir**	**Presentation**	**Peak or nadir**	**Presentation**	**Peak or nadir**
WBC, 4.5-11 × 10^9/L	12.6	12.8	23.3	30.2	WNL	WNL
Hemoglobin, 13.5-17.5 g/dL	11.2	9.9	7.7	4.7	7.7	6.9
Hematocrit, 35%-50%	31.9	27.8	22.8	14.3	23.3	20.4
Platelet count, 150-450 × 10^9/L	43	41	18	13	20	20
Creatinine, 0.6-1.3 mg/dL	WNL	WNL	2.2	5.3	1.6	1.7
LDH, 140-280 U/L	1507	1507	1981	4418	2584	2854
Haptoglobin, 30-200 mg/dL	Undetectable		Undetectable		Undetectable	
ADAMTS13	66%		64%		ND	
D-dimer, ≤0.5 μg/mL	0.97	0.97	ND		ND	
C3, 88-252 mg/dL	45	44	WNL	22	73	69
C4, 12-75 mg/dL	6	6	WNL	5	10	6
CH-50, 31-60 U/mL	24	24	WNL	13	WNL	WNL
Troponin I, <0.01 ng/mL	6.14	6.14	4.95	27.2	12.83	22.53
Hepatitis B antibody	Negative		Negative		Negative	
Hepatitis C antibody	13.73		Negative		Negative	
Echocardiography	EF 55%		EF 30%, mild RV and LV dilation		EF 20%, global hypokinesis, moderate RA dilation	

EF, left ventricular ejection fraction; LV, left ventricular; ND, not determined; RA, right atrial; RV, right ventricular; WNL, result within reference range.

injections of freshly solubilized PEO+ administered once or repeatedly (5 times at 1.5-hour intervals). The plasma level of HMW PEO, the main constituent of the inert ingredient mixture, was determined over time. Single injections of 0.1 mg/kg and 0.3 mg/kg PEO+ resulted in a peak plasma PEO concentration of 3 μg/mL and 5 μg/mL, respectively, which was followed by a slow elimination of PEO from

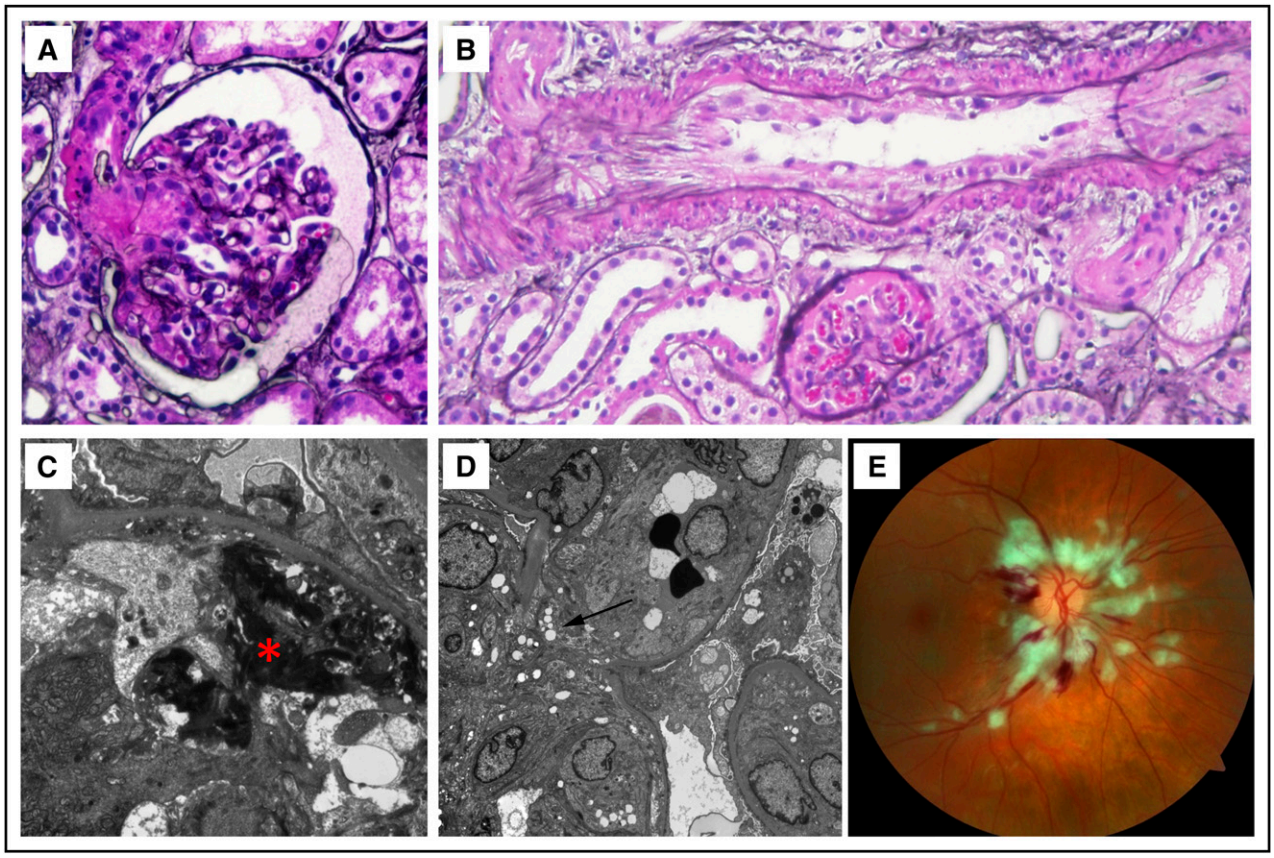

Figure 1. Renal biopsy findings and retinal fundus photograph from patients following IV abuse of extended-release oxymorphone tablets. (A) TMA involving the arteriole with fibrinoid necrosis, extending into the vascular pole of the glomerulus (Jones silver stain, original magnification ×200). (B) Large artery showing endothelial swelling and partial lumen occlusion, with congested glomerulus below (Jones silver stain, original magnification ×100). (C) Fibrin tactoids (red asterisk) underneath swollen endothelium with overlying podocyte foot process effacement, without immune complex deposition (transmission electron microscopy, original magnification ×7100). (D) Swollen endothelium nearly occluding capillary lumen, with RBC fragments (dark black material) and overlying podocyte foot process effacement, without immune complexes. Clear vacuolated areas (black arrow) are found in endothelium and other cells, possibly representing particulate matter from adulterated tablets (transmission electron microscopy, original magnification ×2800). (E) Retinal fundus photograph in a patient experiencing loss of vision following IV abuse of extended-release oxymorphone, demonstrating numerous cotton-wool spots and microhemorrhages.

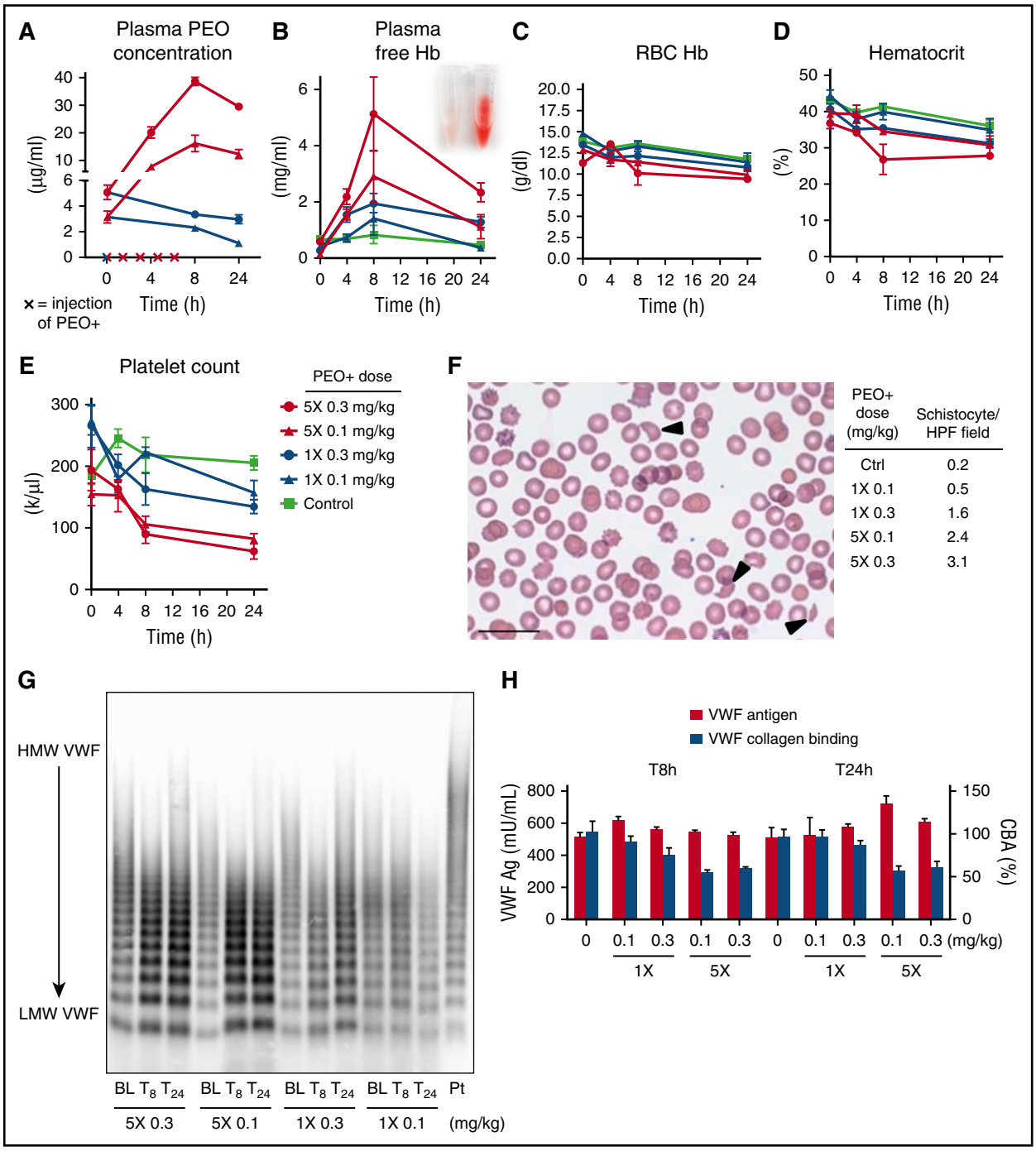

Figure 2. IV PEO+ results in intravascular hemolysis, declines platelet count and the appearance of schistocytes in the peripheral blood accompanied by increased LMW VWF multimers. (A) The plasma PEO concentration of all PEO+ treated groups over time. Multidosed (5 times [5×]) guinea pigs were injected repeatedly with PEO+ at 1.5-hour intervals (as designated on x-axis). (B-E) Hematologic changes in cell free plasma hemoglobin, total RBC hemoglobin, hematocrit, and platelet count in guinea pigs after a single (1×) or repeated (5×) injections of 0.1 and 0.3 mg/kg PEO+. The inset in panel B provides a visualization of the extent of plasma hemoglobin in maximally dosed guinea pigs vs control. (F) Appearance of schistocytes (arrowheads) in blood smears prepared from PEO+ treated animals (modifed Wright-Giemsa stain; scale bar, 20 µm). Quantification of schistocytes in the peripheral blood 24 hours postinjection is presented as number per high power field. (G) The molecular weight distribution of VWF multimers in PEO+ treated guinea pig plasma samples was assessed by low-resolution (0.6%) SDS agarose gel electrophoresis at baseline (BL), 8 hours (T_8) and 24 hours (T_{24}) after injection. Platelet lysate (Pt) prepared from normal guinea pig blood was used as a reference for minimally proteolyzed HMW VWF. (H) VWF antigen and VWF collagen-binding activity in plasma collected at 8 and 24 hours after injection with PEO+. All data displayed as mean values ± SEM (n = 4 per group). Ag, antigen; CBA, collagen-binding activity; Ctrl, control; Hb, hemoglobin; HPF, high powered field; LMW, low-molecular-weight.

the circulation through 48 hours (Figure 2A). Five injections at 1.5-hour intervals resulted in the accumulation of PEO in plasma through the last injection, reaching a maximal concentration of ~15 µg/mL (5 times, 0.1 mg/kg) and ~40 µg/mL (5 times, 0.3 mg/kg) at 8 hours, respectively, followed by a decline in plasma PEO concentration over time.

Following IV administration of PEO+, we observed an abrupt, dose-dependent increase in free hemoglobin in the plasma accompanied

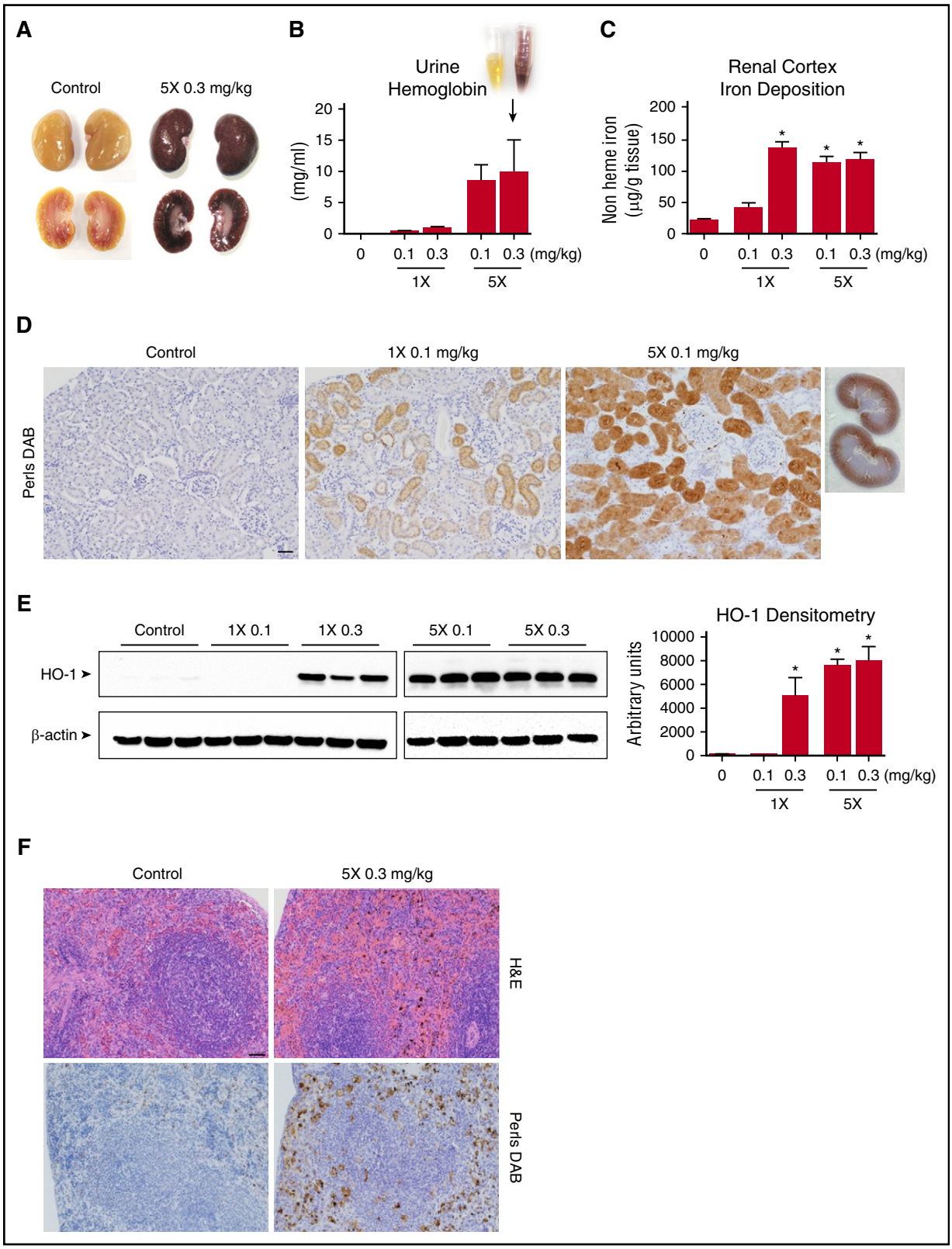

Figure 3. Tissue iron deposition secondary to PEO+ induced hemolysis. (A) High levels of cell free hemoglobin result in macroscopic discoloration of kidneys after exposure to IV PEO+. (B) Quantitation of T_{24h} urine hemoglobin. (C) Quantitation of nonheme bound iron accumulation in the renal cortex of PEO+ injected animals measured by a colorimetric ferrozine-based assay at the study end point. (D) Iron deposition within the renal cortex highlighted by Perls DAB staining. Renal cortical areas are shown from control, single (1×), and multidosed (5×) animals (scale bar, 50 μm), demonstrating the tendency for iron to deposit within the proximal tubule. (E) Western blot of HO-1 expression in kidney tissue and its quantitative densitometric analysis. β-actin was probed as a loading control. (F) Splenic sections stained with H&E and Perls DAB from a multidosed (5×) and control animal (scale bar, 50 μm), demonstrating increased hemosiderin deposition and red cell engorgement. Data displayed as mean values ± SEM (n = 4 per group). *$P < .05$ (1-way ANOVA).

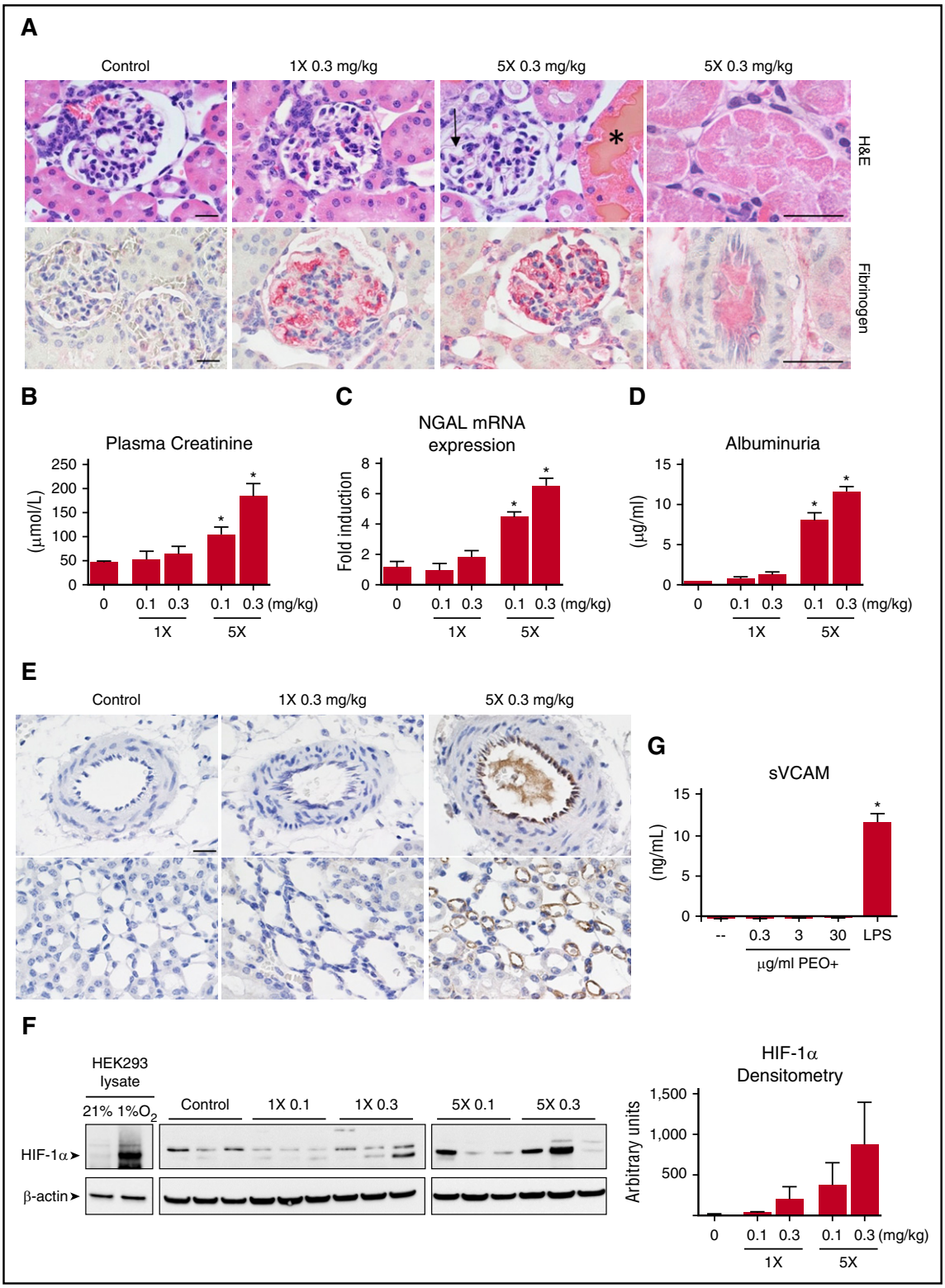

Figure 4. PEO+ induced acute kidney injury and identification of HWM PEO in the microvasculature. (A) Representative kidney sections stained with H&E (top panel) and for fibrinogen by immunohistochemistry (NovaRed, bottom panel) (scale bar, 20 μm). Multidosed (5×) animals demonstrate glomerular capillary swelling (arrow), patchy necrosis of proximal tubule cells with widespread eosinophilic intracellular inclusions (rightmost panel), and hemoglobin laden tubular casts (*). A dose-dependent increase in fibrin deposition within the glomerular capillaries of PEO+ treated animals could be found. (B-D) Quantitation of T_{24h} plasma creatinine levels, renal cortex mRNA NGAL levels, and urinary albumin after PEO+ administration (n = 4 per group). (E) Kidney sections of control, single (1×) and multidosed (5×) PEO+ animals were immunohistochemically stained for PEO using a monoclonal antibody against the polyethylene backbone with DAB development. Interlobular arteries (top panel) and vasa recta lining the loop of Henle (bottom panel) are shown (scale bar, 20 μm). (F) Western blot for HIF-1α expression in the renal cortex of representative animals. β-actin was probed as a protein loading control. Cell lysates of hypoxic (8 hours at 1% O_2) and normoxic (21% O_2) HEK293 cells served as a reference of the HIF-1α–specific upregulated band. (G) HUVECs were cultured for 24 hours in the presence of various concentrations of PEO+ or activated with 1 μg/mL lipopolysaccharide. The amount of sVCAM released into the cell culture supernatant was quantified by ELISA. *$P < .05$ (1-way ANOVA).

by modest declines in total RBC hemoglobin, hematocrit, and platelet count (Figure 2B-E). Maximum plasma free hemoglobin levels were reached 8 hours after the first injection in both single and repeatedly dosed guinea pigs. Peripheral blood smears prepared from PEO+ treated animals revealed the existence of schistocytes, which appeared in the peripheral blood in a dose-dependent manner (Figure 2F). Hemolysis could not be recapitulated by directly spiking PEO+ into control blood subjected to end-over-end mixing, arguing against a direct hemolytic effect (data not shown). Measurements of RBC deformability by ektacytometry were also unaffected by the presence of PEO+ (data not shown). Although a small increase in total leukocyte count was observed in animals injected with the highest dose of PEO+ over control animals (7.1 vs 4.3 $\times$ 10^9/L at 24 hours), the leukocyte count of all animal groups remained within reference ranges.[20]

With evidence of microangiopathic hemolytic anemia and decreased platelet counts, we next characterized the VWF multimer distribution using SDS agarose gel electrophoresis. Hyperreactive, ultra-large multimers of VWF accumulate during the remission phases of ADAMTS13 deficiency–mediated TTP.[14] The plasma of animals injected with PEO+ showed no evidence of increased HMW VWF species (Figure 2G). Increased quantities of low-molecular-weight VWF species were instead seen in multidosed animals, reflected by decreased VWF collagen-binding activity to antigen ratios (Figure 2H). This VWF profile supports a state of TMA[21,22] and high shear stress in the microcirculation,[23-25] which can promote Weibel-Palade body release,[26] platelet-VWF interaction,[27,28] and proteolysis of VWF.[22] No significant differences in D-dimer and complement C3 levels among control and PEO+ injected animals were found, arguing against the occurrence of disseminated intravascular coagulation or complement activation (data not shown).

End-organ changes following IV PEO+ dosing: hemolysis, tissue iron deposition, and response to heme stress

The kidneys of multidosed PEO+ animals were macroscopically found to have a dark brown discoloration of renal cortical tissue (Figure 3A), which is consistent with high levels of hemoglobinuria (Figure 3B). The iron content within the renal cortex tissue of single-dose and multidosed animals was significantly elevated (Figure 3C), depositing primarily within the proximal and distal tubules (Figure 3D). In response to elevated hemoglobin/heme-mediated oxidative stress, the expression of heme oxygenase 1 (HO-1) was found to be significantly upregulated (Figure 3E). The spleen of multidosed animals likewise showed engorgement of the red pulp with red cells and red cell fragments in H&E-stained sections, accompanied by widespread iron/hemosiderin deposits (Figure 3F).

Kidney sections from multidosed animals demonstrated signs of glomerular and tubular damage. Proximal tubular epithelial cells showed hyaline droplet deposition and patchy necrosis, resulting in the filling of tubular lumens with cellular debris and protein casts. Ectatic glomerular capillary loops were frequently seen (Figure 4A top panel). These outcomes were mostly absent in animals given a single injection of PEO+. A dose-dependent increase in glomerular capillary fibrinogen content was also identified by immunohistochemistry (Figure 4A bottom panel). Glomeruli did not stain positively for VWF or platelet antigen (data not shown). These histological findings support the capacity for IV PEO+ to mediate a unique constellation of tubular and glomerular damage with a strong dose dependency (ie, minimal changes with single injections of PEO+ vs overt kidney injury following repeated injections).

To better define the extent of kidney damage, common markers of acute kidney injury were quantified (Figure 4B-D). Only repeatedly dosed groups (5 times, 0.1 mg/kg; and 5 times, 0.3 mg/kg) were found to have significant elevations of plasma creatinine, with twofold and fourfold increases over control at 24 hours, respectively. NGAL (or Lcn2) is rapidly induced and secreted from renal distal tubules following ischemic or nephrotoxic injury.[29,30] The level of NGAL messenger RNA (mRNA) transcript within the renal cortex of multidosed animals (5 times, 0.1 mg/kg; and 5 times, 0.3 mg/kg) was increased by fourfold and sevenfold over control, respectively, whereas guinea pigs receiving single doses of PEO+ showed no significant NGAL upregulation. Significant albuminuria was also observed in repeatedly dosed animals, indicating impaired glomerular permeability function, which may occur secondary to podocyte injury and/or lack of tubular reabsorption of filtered albumin.

Identification of HMW PEO within the renal microvasculature

The distribution of HMW PEO within the kidney following its IV administration was evaluated by immunohistochemistry using an antibody that recognizes the PEO backbone. The endothelium of interlobular arteries as well as the vasa recta (straight capillaries of the medulla) showed positive staining for PEO (Figure 4E top and bottom right panels). The intraluminal appearance of PEO+ material within the small arteries of multidosed animals raised the possibility that microvascular flow or oxygenation may be compromised. We therefore probed the renal cortical tissue by western blot for HIF-1α expression, a transcription factor that mediates adaptive cellular responses to hypoxia. Variable but prominent HIF-1α expression was detected in the renal cortex of multidosed animals, with low levels of HIF-1α expression seen in animals injected with a single 0.3 mg/kg dose (Figure 4F). These results suggest that IV PEO+ may lead to varying degrees of diminished tissue oxygenation. Although this may result in endothelial activation or injury in vivo, the presence of the inert ingredients in the culture medium of HUVECs did not directly stimulate release of sVCAM, a marker of endothelial activation (Figure 4G).

Discussion

Microangiopathic hemolytic anemia, thrombocytopenia, renal injury, and vision loss have been described in prior published cases of TMA associated with extended-release oxymorphone abuse. However, this report introduces the first descriptions of cardiac involvement and atypical clinical features of TMA (eg, pulmonary involvement, dyspnea). Although serum complements were found to be normal in at least 1 other case report,[7] the patients described here were found to have decreasing levels across the course of hospitalization. These declines in complement did not occur concomitant with the onset of disease and, therefore, complement activation/consumption is likely to be of secondary consequence in lieu of a primary mechanism.[31-33] Evidence of foreign material within the plasma of affected individuals was also found. We therefore sought to understand whether the tablet's reformulated inert ingredients could elicit TMA when IV administered to guinea pigs.

IV infusion of the solubilized inert ingredient mixture elicited hallmark features of TMA. Microangiopathic hemolytic anemia, declines in platelet count, and renal injury were all observed with dose dependence in our animal model. These findings speak to the utility of the guinea pig model, which are increasingly recognized for their nephrotoxic sensitivity to hemoglobin[19,34] and also confirm the inert ingredients as a casual factor in the development of TMA.

The injection of HMW PEO (~7 000 000 Da) alone, the main constituent in PEO+ by mass, can recapitulate many of the effects of IV PEO+ at comparable doses (supplemental Figure 1, available on the *Blood* Web site). HMW polymers can decrease disordered motion of RBCs and promote more laminar blood flow.[35] HMW PEO has therefore been investigated as a drag-reducing therapeutic polymer.[36-38] However, recent work has shown that HMW PEO decreases the thickness of the cell-free plasma layer that naturally abuts the microvascular wall, directing RBC traffic more proximal to the vessel wall, thereby generating increased wall shear stress.[39] Our observation of mechanical damage to RBCs and increased proteolysis of VWF support a state of high shear stress in the microvasculature of guinea pigs injected with PEO+. Infusion rate and polymer concentration may be influential in determining the impact of IV HMW PEO, which is reflected in the stepwise gradient of pathology seen in the current animal study. Although shear-driven hemolysis appeared in all animal groups in a dose-dependent manner, end organ damage was only observed in animals given repeated doses. This may also explain why only a minority of individuals (approximately one-third at Wake Forest Baptist Medical Center; P.M., unpublished clinical observations) who seek medical treatment after injecting tablets of extended-release oxymorphone show signs of fulminant TMA.

Renal injury, although seen in many forms of TMA, is also a recognized consequence of acute and chronic hemolysis.[40-43] Brisk hemolysis overwhelms endogenous mechanisms to scavenge free hemoglobin and heme from the circulation,[44] and glomerular filtration becomes a primary mechanism to clear hemoglobin and its decay products. Once outside of the confines of an erythrocyte, hemoglobin can extravasate into tissue compartments where it becomes oxidized and denatured, resulting in heme loss and iron release.[19,45] Hemoglobin degradation products trigger proinflammatory and pro-oxidative cascades[46,47] and cause cytotoxicity through oxidative damage and mitochondrial dysfunction.[46,48-50] Extracellular hemoglobin also readily reacts with numerous small biologic molecules within plasma. Its scavenging of nitric oxide, a potent vasodilator within the microcapillary bed, can result in hypertension and endothelial dysfunction.[50,51] Kidney injury in these cases of TMA is likely a consequence of free hemoglobin toxicity, compromised tissue oxygenation and endothelial injury.

The long-term consequences for renal function in humans have ranged from complete recovery to chronic renal insufficiency necessitating renal replacement therapy. Although the supporting body of evidence is limited, initial plasma exchange therapy has been applied in several cases and may be appropriate in the setting of severe TMA. However, the resolution of symptoms in patients managed with supportive care alone is noteworthy, which may stem from the natural degradation of PEO polymers under flow.[52,53]

Abuse-deterrent formulations are an important mechanism to limit prescription opioid misuse and are part of the FDA's comprehensive action plan to address the public health crisis of opioid addiction, abuse, and overdose.[54] However, the present study demonstrates a potential for HMW PEO–based deterrent formulations to cause hematoxicity, TMA, and end organ injury in the setting of IV misuse. Other oral prescription opioids formulated with HMW PEO have only recently been linked with TMA.[55,56] The reasons for such varying incidence may partially stem from shifting patterns and methods of abuse, but are poorly understood. Although injection abuse of prescription opioids is highly concentrated in certain regions of the United States, particularly in rural Appalachia,[57] all physicians should be highly inquisitive of IV drug abuse when presented with cases of TMA.

Acknowledgments

The authors thank Dan Mellon and Judith Racoosin (Division of Anesthesia, Analgesia, and Addiction Products/Center for Drug Evaluation and Research) for their insightful comments and guidance.

Authorship

Contribution: R.H., A.Y., T.S., A.W., P.W.B., and C.K.-S. designed the study; R.H., A.Y., J.H.B., E.W., and P.W.B. performed experiments; J.T. and P.M. provided case reports and clinical insight; A.B.F. and H.Y. prepared and interpreted human kidney biopsies; and R.H., A.Y., J.T., A.B.F., P.M., P.W.B. and C.K.-S. wrote the manuscript.

Conflict-of-interest disclosure: E.W. is employed by Quest Diagnostics. The remaining authors declare no competing financial interests.

ORCID profiles: R.H., 0000-0003-1418-9919; A.Y., 0000-0002-0203-9297.

Correspondence: Paul W. Buehler, Laboratory of Biochemistry and Vascular Biology, DBCD/OBRR/CBER, FDA, 10903 New Hampshire Ave, Building 52/72, Room 4108, Silver Spring, MD 20993; e-mail: paul.buehler@fda.hhs.gov; and Chava Kimchi-Sarfaty, Hemostasis Branch, DPPT/OTAT/CBER, FDA, 10903 New Hampshire Ave, Building 52/72, Room 4118, Silver Spring, MD 20993; e-mail: chava.kimchi-sarfaty@fda.hhs.gov.

References

1. Rudd RA, Aleshire N, Zibbell JE, Gladden RM. Increases in drug and opioid overdose deaths–United States, 2000-2014. *MMWR Morb Mortal Wkly Rep*. 2016;64(50-51):1378-1382.
2. Centers for Disease Control and Prevention (CDC). Thrombotic thrombocytopenic purpura (TTP)-like illness associated with intravenous Opana ER abuse–Tennessee, 2012. *MMWR Morb Mortal Wkly Rep*. 2013; 62(1):1-4.
3. Rane M, Aggarwal A, Banas E, Sharma A. Resurgence of intravenous Opana as a cause of secondary thrombotic thrombocytopenic purpura. *Am J Emerg Med*. 2014; 32(8):951.
4. Miller PJ, Farland AM, Knovich MA, Batt KM, Owen J. Successful treatment of intravenously abused oral Opana ER-induced thrombotic microangiopathy without plasma exchange. *Am J Hematol*. 2014;89(7):695-697.
5. Amjad AI, Parikh RA. Opana-ER used the wrong way: intravenous abuse leading to microangiopathic hemolysis and a TTP-like syndrome. *Blood*. 2013;122(20):3403.
6. Shah RJ, Cherney EF. Diffuse retinal ischemia following intravenous crushed oxymorphone abuse. *JAMA Ophthalmol*. 2014;132(6):780-781.
7. Ambruzs JM, Serrell PB, Rahim N, Larsen CP. Thrombotic microangiopathy and acute kidney injury associated with intravenous abuse of an oral extended-release formulation of oxymorphone hydrochloride: kidney biopsy findings and report of 3 cases. *Am J Kidney Dis*. 2014;63(6):1022-1026.
8. Jabr FI, Yu L. Thrombotic microangiopathy associated with Opana ER intravenous abuse: a case report. *J Med Liban*. 2016;64(1):40-42.
9. Conrad C, Bradley HM, Broz D, et al; Centers for Disease Control and Prevention (CDC). Community outbreak of HIV infection linked to injection drug use of oxymorphone–Indiana, 2015. *MMWR Morb Mortal Wkly Rep*. 2015;64(16): 443-444.
10. George JN, Nester CM. Syndromes of thrombotic microangiopathy. *N Engl J Med*. 2014;371(19): 1847-1848.
11. Fujikawa K, Suzuki H, McMullen B, Chung D. Purification of human von Willebrand factor-cleaving protease and its identification as a new member of the metalloproteinase family. *Blood*. 2001;98(6):1662-1666.

12. Gerritsen HE, Robles R, Lämmle B, Furlan M. Partial amino acid sequence of purified von Willebrand factor-cleaving protease. *Blood*. 2001; 98(6):1654-1661.
13. Levy GG, Nichols WC, Lian EC, et al. Mutations in a member of the ADAMTS gene family cause thrombotic thrombocytopenic purpura. *Nature*. 2001;413(6855):488-494.
14. Moake JL, Rudy CK, Troll JH, et al. Unusually large plasma factor VIII:von Willebrand factor multimers in chronic relapsing thrombotic thrombocytopenic purpura. *N Engl J Med*. 1982; 307(23):1432-1435.
15. US Food and Drug Administration. FDA Statement: Original Opana ER Relisting Determination. http://www.fda.gov/Drugs/DrugSafety/ucm351357.htm. Accessed 7 July 2016.
16. Smyth HF Jr, Weil CS, Woodside MD, Knaak JB, Sullivan LJ, Carpenter CP. Experimental toxicity of a high molecular weight poly(ethylene oxide). *Toxicol Appl Pharmacol*. 1970;16(2):442-445.
17. Karpova GV, Abramova EV, Lamzina TI, Timina EA, Vetoshkina TV. [Myelotoxicity of high-molecular-weight poly(ethylene oxide)]. *Eksp Klin Farmakol*. 2004;67(6):61-65.
18. Baek JH, Zhou Y, Harris DR, Schaer DJ, Palmer AF, Buehler PW. Down selection of polymerized bovine hemoglobins for use as oxygen releasing therapeutics in a guinea pig model. *Toxicol Sci*. 2012;127(2):567-581.
19. Deuel JW, Schaer CA, Boretti FS, et al. Hemoglobinuria-related acute kidney injury is driven by intrarenal oxidative reactions triggering a heme toxicity response. *Cell Death Dis*. 2016;7: e2064.
20. Hein J, Hartmann K. Labordiagnostische referenzbereiche bei meerschweinchen. *Tieraerztl Prax*. 2003;31:383-389.
21. Mannucci PM, Lombardi R, Lattuada A, et al. Enhanced proteolysis of plasma von Willebrand factor in thrombotic thrombocytopenic purpura and the hemolytic uremic syndrome. *Blood*. 1989; 74(3):978-983.
22. Tsai HM, Sussman II, Nagel RL. Shear stress enhances the proteolysis of von Willebrand factor in normal plasma. *Blood*. 1994;83(8):2171-2179.
23. Blackshear JL, Schaff HV, Ommen SR, Chen D, Nichols WL. Hypertrophic obstructive cardiomyopathy, bleeding history, and acquired von Willebrand syndrome: response to septal myectomy. *Mayo Clin Proc*. 2011;86(3):219-224.
24. Yoshida K, Tobe S, Kawata M, Yamaguchi M. Acquired and reversible von Willebrand disease with high shear stress aortic valve stenosis. *Ann Thorac Surg*. 2006;81(2):490-494.
25. Vincentelli A, Susen S, Le Tourneau T, et al. Acquired von Willebrand syndrome in aortic stenosis. *N Engl J Med*. 2003;349(4):343-349.
26. Galbusera M, Zoja C, Donadelli R, et al. Fluid shear stress modulates von Willebrand factor release from human vascular endothelium. *Blood*. 1997;90(4):1558-1564.
27. Moake JL, Turner NA, Stathopoulos NA, Nolasco L, Hellums JD. Shear-induced platelet aggregation can be mediated by vWF released from platelets, as well as by exogenous large or unusually large vWF multimers, requires adenosine diphosphate, and is resistant to aspirin. *Blood*. 1988;71(5):1366-1374.
28. Moake JL, Turner NA, Stathopoulos NA, Nolasco LH, Hellums JD. Involvement of large plasma von Willebrand factor (vWF) multimers and unusually large vWF forms derived from endothelial cells in shear stress-induced platelet aggregation. *J Clin Invest*. 1986;78(6):1456-1461.
29. Devarajan P. Neutrophil gelatinase-associated lipocalin (NGAL): a new marker of kidney disease. *Scand J Clin Lab Invest Suppl*. 2008;241:89-94.
30. Bennett M, Dent CL, Ma Q, et al. Urine NGAL predicts severity of acute kidney injury after cardiac surgery: a prospective study. *Clin J Am Soc Nephrol*. 2008;3(3):665-673.
31. Frimat M, Tabarin F, Dimitrov JD, et al. Complement activation by heme as a secondary hit for atypical hemolytic uremic syndrome. *Blood*. 2013;122(2):282-292.
32. Gordon RJ, Lowy FD. Bacterial infections in drug users. *N Engl J Med*. 2005;353(18):1945-1954.
33. Thorlacius S, Mollnes TE, Garred P, et al. Plasma exchange in myasthenia gravis: changes in serum complement and immunoglobulins. *Acta Neurol Scand*. 1988;78(3):221-227.
34. Cui J, Bai XY, Sun X, et al. Rapamycin protects against gentamicin-induced acute kidney injury via autophagy in mini-pig models. *Sci Rep*. 2015; 5:11256.
35. Kameneva MV, Polyakova MS, Fedoseeva EV. Effect of drag-reducing polymers on the structure of the stagnant zones and eddies in models of constricted and branching blood vessels. *Fluid Dynamics*. 1990;25(6):956-959.
36. Golub AS, Grigorian MR, Kameneva MV, Malkina NA, Shoshenko KA. Influence of polyethylene oxide on the capilllary blood flow in the diabetic rat. *Sov Phys Dokl*. 1987;32:620-621.
37. Grigorian SS, Kameneva MV, Shakhnazarov AA. Effect of high molecular weight compounds dissolved in blood on hemodynamics. *Sov Phys Dokl*. 1976;21:702-703.
38. Pacella JJ, Kameneva MV, Csikari M, Lu E, Villanueva FS. A novel hydrodynamic approach to the treatment of coronary artery disease. *Eur Heart J*. 2006;27(19):2362-2369.
39. Marhefka JN, Zhao R, Wu ZJ, Velankar SS, Antaki JF, Kameneva MV. Drag reducing polymers improve tissue perfusion via modification of the RBC traffic in microvessels. *Biorheology*. 2009;46(4):281-292.
40. Billings FT 4th, Ball SK, Roberts LJ 2nd, Pretorius M. Postoperative acute kidney injury is associated with hemoglobinemia and an enhanced oxidative stress response. *Free Radic Biol Med*. 2011; 50(11):1480-1487.
41. Ballarín J, Arce Y, Torra Balcells R, et al. Acute renal failure associated to paroxysmal nocturnal haemoglobinuria leads to intratubular haemosiderin accumulation and CD163 expression. *Nephrol Dial Transplant*. 2011;26(10): 3408-3411.
42. Qian Q, Nath KA, Wu Y, Daoud TM, Sethi S. Hemolysis and acute kidney failure. *Am J Kidney Dis*. 2010;56(4):780-784.
43. Vermeulen Windsant IC, Snoeijs MG, Hanssen SJ, et al. Hemolysis is associated with acute kidney injury during major aortic surgery. *Kidney Int*. 2010;77(10):913-920.
44. Muller-Eberhard U, Javid J, Liem HH, Hanstein A, Hanna M. Plasma concentrations of hemopexin, haptoglobin and heme in patients with various hemolytic diseases. *Blood*. 1968;32(5):811-815.
45. Schaer DJ, Buehler PW, Alayash AI, Belcher JD, Vercellotti GM. Hemolysis and free hemoglobin revisited: exploring hemoglobin and hemin scavengers as a novel class of therapeutic proteins. *Blood*. 2013;121(8):1276-1284.
46. Baek JH, Zhang X, Williams MC, Schaer DJ, Buehler PW, D'Agnillo F. Extracellular Hb enhances cardiac toxicity in endotoxemic guinea pigs: protective role of haptoglobin. *Toxins (Basel)*. 2014;6(4):1244-1259.
47. Schaer CA, Deuel JW, Bittermann AG, et al. Mechanisms of haptoglobin protection against hemoglobin peroxidation triggered endothelial damage. *Cell Death Differ*. 2013;20(11): 1569-1579.
48. Baek JH, D'Agnillo F, Vallelian F, et al. Hemoglobin-driven pathophysiology is an in vivo consequence of the red blood cell storage lesion that can be attenuated in guinea pigs by haptoglobin therapy. *J Clin Invest*. 2012;122(4): 1444-1458.
49. Schaer DJ, Buehler PW. Cell-free hemoglobin and its scavenger proteins: new disease models leading the way to targeted therapies. *Cold Spring Harb Perspect Med*. 2013;3(6):a013433.
50. Schaer DJ, Vinchi F, Ingoglia G, Tolosano E, Buehler PW. Haptoglobin, hemopexin, and related defense pathways-basic science, clinical perspectives, and drug development. *Front Physiol*. 2014;5:415.
51. Schaer CA, Deuel JW, Schildknecht D, et al. Haptoglobin preserves vascular nitric oxide signaling during hemolysis. *Am J Respir Crit Care Med*. 2016;193(10):1111-1122.
52. Fisher DH, Rodriguez F. Degradation of drag-reducing polymers. *J Appl Polym Sci*. 1971; 15(12):2975-2985.
53. Marhefka JN, Velankar SS, Chapman TM, Kameneva MV. Mechanical degradation of drag reducing polymers in suspensions of blood cells and rigid particles. *Biorheology*. 2008;45(5): 599-609.
54. Califf RM, Woodcock J, Ostroff S. A proactive response to prescription opioid abuse. *N Engl J Med*. 2016;374(15):1480-1485.
55. Tate C, Mollee P. Intravenous oxycontin-associated thrombotic microangiopathy treated successfully without plasma exchange. *Med J Aust*. 2015;202(6):330-331.
56. Nataatmadja M, Divi D. Relapsing thrombotic microangiopathy and intravenous sustained-release oxycodone. *Clin Kidney J*. 2016;9(4): 580-582.
57. Young AM, Havens JR, Leukefeld CG. Route of administration for illicit prescription opioids: a comparison of rural and urban drug users. *Harm Reduct J*. 2010;7:24.